Regular article

Generalized reaction-path Hamiltonian dynamics*

Javier González[1,3], **Xavier Giménez**[1,3], **Josep Maria Bofill**[2,3]

[1] Departament de Química Física, Universitat de Barcelona, Martí i Franquès 1, 08028, Barcelona, Catalunya, Spain
[2] Departament de Química Orgànica, Universitat de Barcelona, Martí i Franquès 1, 08028, Barcelona, Catalunya, Spain
[3] Centre especial de Recerca en Química Teòrica, Parc Científic de Barcelona, 08028, Barcelona, Catalunya, Spain

Abstract. The reaction-path Hamiltonian is reformulated in a form that is independent of the specific choice of guiding path. A necessary and sufficient condition for a given curve to satisfy reaction-path Hamiltonian requirements is derived, showing that any curve with no explicit dependence on the independent parameter does give rise to a formally acceptable reaction-path Hamiltonian. Numerical calculations have also been performed, comparing some reaction-path choices with the exact classical dynamics, evidencing the physically ground basis of most reaction path approaches.

Keywords: Reaction-path Hamiltonian – Reaction path – Classical dynamics – Molecular dynamics

Introduction

The concept of reaction paths is a celebrated one. It has found widespread use in descriptions of reaction mechanisms, which are based on geometrical rearrangements of the atoms comprising a given chemical system [1]. More specifically, reaction path terminology is linked to the path described on a multidimensional, configuration space potential-energy surface, when the transformation from reactants to products is considered. This use of configuration space instead of phase space obviously means neglecting the contribution of the kinetic energy of the nuclei, so establishing the specific path described by any real rearrangement event turns out to be somewhat ambiguous. This ambiguity is not removed even after considering that the guiding premise should be the likely evolution of the system toward lower potential

energy. In chemical reactions this is certainly not the case, for at least half of the collisions between reactants and transition states usually at higher potential energy. Thus the initial conditions corresponding to the kinetic energy of the nuclei critically determine the true specific, undulating path evolving from favourably oriented reactants towards the transition state bottleneck and then to products. In bulk systems myriads of initial conditions are necessary to reasonably mimic the experimental conditions, so that even under the assumption of partial equilibrium conditions the problem that arises is, at the very least, cumbersome. One can resort to the Liouville theorem and then solve for the classical density, but its use merely halves the dimensionality problem [2, 3].

These premises may partially explain why description of chemical reactions has so frequently been kept in purely geometrical terms. An effort to incorporate the dynamic information while, at the same time, keeping the simplicity of envisaging the reaction as a single path on the potential energy surface, was introduced with the formulation of the reaction-path Hamiltonian (RPH) [4]. This views the reaction as a vibrating super-molecule, for which some distances undergo dramatic changes, those most properly describing the reaction, whereas the remaining degrees of freedom experience some changes in the nature of the associated vibrational motion. This latter feature mathematically translates into a set of couplings between the successive normal mode expansions in which the complete reaction path is subdivided. A key aspect is that reaction is most properly described in terms of a "distinguished", large amplitude *normal mode*. This means that, physically, the true reaction is a concerted, strongly correlated motion involving, in principle, all atoms of the system. Thus, the mathematical one-dimensional reaction path is actually a non-local motion whose (sometimes) imaginary frequency suffers strong variation when going from reactants to products [5]. When the reaction path bifurcates, the saddle point is of higher order or the passage from

---

*Dedicated to Professor S. Olivella in his 60th birthday

Correspondence to: Josep M. Bofill
e-mail: jmbofill:qo.ub.es

reactants to products is described by a strongly skewed surface; several higher-dimensional variants of the reaction path, namely the reaction surface or the reaction-volume Hamiltonian, have been proposed and tested [6, 7, 8, 9].

A further reformulation, concerning the arc length associated to the reaction path co-ordinate, plus a linear Taylor expansion of the gradient equation defining the guiding path led, more recently, to an efficient formulation of the reaction-path Hamiltonian [10]. In particular, the number of grid points necessary for a converged description of the reaction-path Hamiltonian dynamics turns out to be substantially reduced. This feature is attributable to the fact that the first order in the gradient expansion, instead of zero order, is fully incorporated into the complete set of dynamic equations. Interestingly, the linear expansion of the gradient ultimately leads (i.e. after some algebra) to a Bernoulli-type differential equation, inside the validity range for each quadratic expansion of the potential energy surface along the reaction path.

In spite of the previous considerations, an essential basic ambiguity still prevails in any reaction path description, either structural or dynamic, of a chemical reaction. This ambiguity is, namely, the selection of the specific reference path into which one constrains the molecular system to evolve, a selection which is easily recognized to certainly incorporate an ad hoc component. If one does not go further in the level of theory, so that one keeps the economy of the reaction path idea, no formal arguments give priority to a given path over another. One can thus focus on paths accomplishing some particular topological properties, or on those arising from defining differential equations that exhibit improved properties when dealing with some regions of the potential energy surface. This issue has been recently considered by the authors. In particular, a Newton path (NP) proved superior, when dealing with bifurcation points, than the more traditional Intrinsic reaction coordinate path (IRC) [11]. The reaction dynamics emerging from both paths evidenced some differences, even though they were ultimately not substantial when all degrees of freedom where globally compared.

This latter feature, along with the strong formal parallelism between the IRC and the Newton RPH formulations, prompted a further study, namely definition of a reaction-path Hamiltonian in terms of a reference path, which is defined in much more general terms than previous formulations. It has been found that this is not only possible, but that a formal, elegant way of deriving the dynamic equations of motion emerges; it is, in addition, much more straightforward. The purpose of this article is thus to show this formulation of the generalized reaction-path Hamiltonian dynamics. In addition, some numerical tests have been performed, aimed at showing that any of the specific formulations of the reaction-path Hamiltonian dynamics yields both position and momentum time dependencies that are in global, physical good agreement with exact classical dynamics. It thus provides

a necessary test prior to extending these reaction-path Hamiltonian formulations to their application to large polyatomic systems.

The article is organized as follows: first we discuss the problem and derive the generalized reaction-path Hamiltonian. Numerical results, corresponding to a model reference system, showing the physical basis of the reaction path idea, are shown next. Finally, some conclusions are given.

Theoretical approach: the parametric form of the Euler–Lagrange equations as a basis for the general formulism of the reaction-path Hamiltonian

The basic idea of the reaction-path Hamiltonian, RPH, as stated, is to constrain the motion of a molecule along a determined path or curve in configuration space. These dynamics take into account both the motion through the reaction path and the harmonic deviations along it. A well-known, pioneering version of the RPH was derived by Miller, Handy and Adams (MHA) some years ago [4]. Essentially, their Hamiltonian is a generalization of the natural collision coordinate Hamiltonian for collinear systems [12], to molecules with many degrees of freedom. In fact it was obtained by adapting "the large amplitude motion" Hamiltonian of a "floppy" degree of freedom, for which an anharmonic treatment is considered. This large amplitude motion coordinate is the reaction coordinate. The main drawback of this RPH derivation is that the resulting equations of motion cannot be integrated easily, owing to the explicit appearance of the couplings between the reaction coordinate and the other harmonic coordinates in the system Hamiltonian. The restricted nature (i.e. harmonic-like) of the molecular motion perpendicular to the reference curve or reaction coordinate is the origin of these couplings, since the nature of the perpendicular harmonic motion substantially changes as one advances along the reaction coordinate.

An alternate way to address the formulation of the RPH was considered by González, Giménez, and Bofill (hereafter termed as GGB-RPH) [10]. The basic idea consists in parameterization of the curve, or reaction path, the parameter being the reaction coordinate or arc length. All the coordinates that characterize the reaction path are then a function of the reaction coordinate. Consequently, any motion along the path implies a change in this reaction coordinate. When the parameterization of the curve consists in assuming that the RP follows the intrinsic reaction coordinate, IRC, the defining equation is [13, 14, 15]:

$$\frac{d\Delta\mathbf{q}_0}{ds} = \frac{\mathbf{g}(\Delta\mathbf{q}_0(s))}{\sqrt{[\mathbf{g}(\Delta\mathbf{q}_0(s))]^T \mathbf{g}(\Delta\mathbf{q}_0(s))}} \tag{1}$$

where $\Delta\mathbf{q}_0 = \mathbf{q} - \mathbf{q}_0$ and $\mathbf{g}$ are the corresponding mass-weighted internal coordinates and gradient vectors, respectively. For a strict definition of $\mathbf{q}$ and $\mathbf{q}_0$, see Ref. [10]. The first order differential equation Eq. (1)

defines the tangent of the IRC in internal coordinates, whereas the parameter s plays the role of an arc length. The above IRC is a parametrically defined curve in the M-dimensional mass-weighted internal coordinate space, where $M = 3N-6$, and N is the number of atoms of the supermolecule.

The mathematical equations for the path lead to a stepwise integration, analytic inside each quadratic region into which the reaction coordinate can be divided. An important feature of the GGB-RPH formulation is that the range of validity of the quadratic expansion gets very much enlarged in this new version, owing to the linear expansion of the gradient differential equation defining the reference path, instead of the zeroth order used by MHA in their original derivation. Therefore, substituting the equations of the path, as a function of the reaction coordinate, into a classical Hamiltonian yields a new form of RPH. The associated equations of motion of this RPH are easily solvable because the couplings between the harmonic coordinates, belonging to different quadratic expansions, appear implicitly. Consequently, this new RPH depends only on a position coordinate and its conjugate momentum, rather than on the whole set of M coordinates and their conjugate momenta. The above transformations, along with some further re-parameterizations, introduced to simplify the final equations of motion, lead to a Bernouilli-type dynamic equation [10]:

$$\frac{d\chi}{dt} + a\chi^2 + 1 = 0 \tag{2}$$

where the final unknown function is derived after the following consecutive transformations: $u(s) = \exp\left\{\alpha \int_{s_0}^{s} \frac{1}{\sqrt{g^T g}} ds'\right\}$, $u = \exp(\tau)$, $\chi = d\tau/dt$, with the proportionality constant α having units of $energy \times length^{-2}$. In Eq. (2), $a = (g_0)^T H_0 g_0/(g_0)^T g_0 - 1$, where g_0 and H_0 are, respectively, the gradient vector and the Hessian matrix in mass-weighted internal coordinates at the reference point for the quadratic expansion. Once solved (i.e. once $u(t)$ and the conjugate momentum, $p_u(t)$, are available for all relevant t), one may easily recover the dynamics associated to the original normal mode coordinates through the relation:

$$q(u) = q_0 - \left(I - u^{H_0}\right)H_0^{-1}g_0 \tag{3}$$

As stated in the Introduction, the above RPH derivation has some flexibility concerning the precise definition of the reference path. In particular, it has been shown that proceeding closely in parallel to the algebra leading to the IRC-RPH, it is possible to easily derive a Newton-RPH [11]. This variant shows the advantage of naturally dealing with valley-ridged inflection (VRI) points (i.e. it removes the ambiguity in deciding the direction of further advance when the path crosses a VRI). This advantage arises thanks to the inclusion of the Hessian in the defining differential equation for the Newton following algorithm [16]:

$$\frac{dq(s)}{ds} = \pm A[q(s)]g[q(s)] \tag{4}$$

where A is the adjoint matrix of the Hessian matrix H. Thus, one has algorithmically available all the frequencies across a VRI point, which is precisely the kind of information missing in IRC-following algorithms. It is then trivial, by inspection of the two imaginary frequencies, to select the larger absolute value and proceed ahead along the reaction coordinate. The final equations of motion, obtained again after suitable re-parameterizations, look very similar to those characterizing the IRC-RPH equations of motion:

$$\frac{d\chi}{dt} + \overline{a}\chi^2 + b = 0 \tag{5}$$

where $\overline{a} = \det(H_0)$, $b = k/\overline{a}m$, with $k = g_0^T H_0^{-1} g_0$ and $m = g_0^T H_0^{-2} g_0$. The consecutive transformations in the independent parameter that lead to Eq. (5) are now $ds/d\tau = \left\{(g_0 + H_0\Delta q_0)^T A^2 (g_0 + H_0\Delta q_0)\right\}$, $u(\tau) = \exp\left\{\det(H_0)\tau\right\}$, and $\chi = d\tau/dt$. Finally, the relations linking the reaction path dynamic variable u to the original normal mode coordinates is now:

$$q(u) = q_0 - (1-u)H_0^{-1}g_0 \tag{6}$$

Thus, Eqs (2) and (3) for the IRC look remarkably similar to Eqs (5) and (6) for the Newton Path, even though the algebraic transformations within each derivation are substantially different in detail. In particular, one should notice that, for the IRC, u is defined in terms of s, whereas for the NP is τ the parameter defined in terms of s. Then, in both cases a relation between τ and u leads to dynamic equations in Hamiltonian form, for the reduced u, p_u pair of phase space variables.

This possibility, namely the capability of the GGB-RPH to handle several definitions of the reference path, strongly suggests that a more general RPH formulation, in terms of generalized properties of the reaction path, might be possible. It is clear, from the above considerations, that both the starting equation, defining the parametric curve on the PES, and the re-parameterization sequence necessary to yield the final equations of motion in Hamiltonian form are going to play a key role in this general discussion. Actually, one may state our main goal in the following form: Which are the minimum requirements, for a given path and any possible re-parameterization of it, to obtain a final, *reduced* set of dynamic equations in Hamiltonian form?

Next we present this generalized class of RPH, its derivation being based on the parametric form of the calculus of variations [17]. The main conclusion, quite remarkable, to be extracted is that the general expression enables the derivation of an RPH for *any* type of path, assuming the associated Lagrangian functional is not *explicitly* dependent on the curve parameter.

The derivation begins by considering that the classical motion of a molecular system of N atoms, during the

time interval $[t_0, t]$, is assumed to be described by a curve function $\mathbf{q}(t)$ for which the action integral [18]:

$$J[\mathbf{q}] = \int_{t_0}^{t} L\left(\mathbf{q}, \frac{d\mathbf{q}}{dt}\right) dt = \int_{t_0}^{t} \left[\frac{1}{2}\left(\frac{d\mathbf{q}}{dt}\right)^T \left(\frac{d\mathbf{q}}{dt}\right) - V(\mathbf{q})\right] dt \tag{7}$$

is a minimum. In Eq. (7), $\mathbf{q}$ is the mass–weighted vector internal coordinate and $V(\mathbf{q})$ the potential function. A key aspect of our derivation is that we are seeking the general criteria for any curve parameterization to be acceptable as a RP, i.e. that it is capable of yielding a proper RPH. To that purpose, a prospectively good strategy might seem to formulate the least action principle in terms of an explicit dependence on the curve *parameterization* (but not an explicit dependence on the parameter itself). This means that one must change the independent variable, keeping the path definition (in the $d\mathbf{q}/ds$ form) explicit in the Lagrangian. Eq. (7) can thus be written as:

$$
\begin{aligned}
J[\mathbf{q}] &= \int_{t_0}^{t} L\left(\mathbf{q}, \frac{d\mathbf{q}}{dt}\right) dt \\
&= \int_{s_0}^{s} \left[\frac{1}{2}\left(\frac{d\mathbf{q}}{ds}\right)^T \left(\frac{d\mathbf{q}}{ds}\right)\left(\frac{dt}{ds}\right)^{-1} - \left(\frac{dt}{ds}\right) V(\mathbf{q})\right] ds \\
&= \int_{s_0}^{s} F\left(\mathbf{q}, \frac{d\mathbf{q}}{ds}, \frac{dt}{ds}\right) ds
\end{aligned}
\tag{8}
$$

where the functional F appearing on the right-hand side of Eq. (8) depends on two unknown functions, $\mathbf{q}(s)$ and $t(s)$, where s is the parameter that characterizes the curve. It is easily shown that, in order to obtain acceptable solutions, the functional F must not involve s *explicitly*. Moreover, the functional F is positive-homogeneous of degree one with respect to the arguments $d\mathbf{q}/ds$ and dt/ds. As a consequence of these features, the value of this functional F does not depend on the choice of the parameter, but rather on the nature of the parametric curve line defined in the $\mathbf{q}t$-plane. These statements rest on the basis of Noether's theorem, thus providing a rigorous mathematical link between the present derivation and the Lagrangian mechanics over differentiable varieties [18]. The above requirement may be expressed, in more specific terms, by stating that an explicit dependence on the curve parameter should lead to a non-conserved first integral of the equations of motion, e.g. to non-conservation of energy when the independent parameter plays the role of time, etc...

The variational problem for the right-hand side of Eq. (8) leads to a set of Euler equations:

$$\left[\frac{\partial F}{\partial t} - \frac{d}{ds}\left(\frac{\partial F}{\partial \dot{t}}\right)\right] = 0, \left[\nabla_\mathbf{q} F - \frac{d}{ds}\left(\nabla_{\dot{\mathbf{q}}} F\right)\right] = \mathbf{0} \tag{9}$$

where it is important to note, for the sake of generality, that the overdot indicates differentiation with respect to s. The set of equations Eq. (9) must be equivalent to the single Euler equation corresponding to the variational problem for the original functional given in Eq. (8), namely:

$$\left[\nabla_\mathbf{q} L - \frac{d}{dt}\left(\nabla_{\dot{\mathbf{q}}} L\right)\right] = \mathbf{0} \tag{10}$$

where now the overdot obviously means differentiation with respect to time. Consequently, the set of equations Eq. (9) cannot be independent, and it is possible to show that they are connected by the identity [17]:

$$\frac{dt}{ds}\left[\frac{\partial F}{\partial t} - \frac{d}{ds}\left(\frac{\partial F}{\partial \dot{t}}\right)\right] + \left(\frac{d\mathbf{q}}{ds}\right)^T \left[\nabla_\mathbf{q} F - \frac{d}{ds}\left(\nabla_{\dot{\mathbf{q}}} F\right)\right] = 0 \tag{11}$$

assuming $dt/ds \neq 0$ and $d\mathbf{q}/ds \neq 0$. Using Eq. (8), the first term on the left hand side of Eq. (11) leads to:

$$\frac{d}{ds}\left[\frac{1}{2}\frac{(d\mathbf{q}/ds)^T (d\mathbf{q}/ds)}{(dt/ds)^2} + V(\mathbf{q})\right] = 0 \tag{12}$$

Eq. (12) tells us that the total energy is constant through the parametric curve $\mathbf{q} = \mathbf{q}(s)$, $t = t(s)$. This total energy may then be written in a more convenient form:

$$E = \frac{1}{2}\left(\frac{d\mathbf{q}}{ds}\right)^T \left(\frac{d\mathbf{q}}{ds}\right)\left(\frac{ds}{dt}\right)^2 + V(\mathbf{q}) \tag{13}$$

The second term on the left hand side of Eq. (11) is related to the parametric nature of the curve line. However in the present study, since this curve is imposed rather than an extremal of the action integral Eq. (8), either the second expression of Eq. (9) or the second term on the left hand side part of Eq. (11), is not satisfied in general. The general RPH is derived defining the conjugate momentum to the reaction coordinate, now represented by the s parameter:

$$p_s = \left(\frac{d\mathbf{q}}{ds}\right)^T \left(\frac{d\mathbf{q}}{ds}\right)\left(\frac{ds}{dt}\right) \tag{14}$$

and taking into account Eq. (13) and the curve $\mathbf{q} = \mathbf{q}(s)$:

$$H(s, p_s) = \frac{1}{2}\frac{p_s^2}{\left(\frac{d\mathbf{q}}{ds}\right)^T \left(\frac{d\mathbf{q}}{ds}\right)} + V[\mathbf{q}(s)] \tag{15}$$

It is worth noting that the factor $\left(\frac{d\mathbf{q}}{ds}\right)^T \left(\frac{d\mathbf{q}}{ds}\right)$ plays in this formulation the role of a mass, although it is a variable term as one advances along the reaction coordinate. One may then envision the resulting one-dimensional effective motion as a time evolution of a particle, under the potential given by $V[\mathbf{q}(s)]$, but with variable inertia. This view has an interesting parallelism

with the RPH covariant formulation of Okuno [26], as one may identify his g^{ss} metric tensor component with the inverse of $\left(\dfrac{d\mathbf{q}}{ds}\right)^{T}\left(\dfrac{d\mathbf{q}}{ds}\right)$.

Finally, applying Hamilton's equation of motion to Eq. (15), we obtain the time-evolution differential equations for both s and p_s:

$$\frac{ds}{dt} = \frac{p_s}{\left(\dfrac{d\mathbf{q}}{ds}\right)^{T}\left(\dfrac{d\mathbf{q}}{ds}\right)}$$

$$\frac{dp_s}{dt} = -\frac{\partial H(s,\,p_s)}{\partial s} = p_s^2 \frac{\left(\dfrac{d\mathbf{q}}{ds}\right)^{T}\left(\dfrac{d^2\mathbf{q}}{ds^2}\right)}{\left[\left(\dfrac{d\mathbf{q}}{ds}\right)^{T}\left(\dfrac{d\mathbf{q}}{ds}\right)\right]^2}$$
$$- \left(\frac{d\mathbf{q}}{ds}\right)^{T}\nabla_{\mathbf{q}}V[\mathbf{q}(s)] \qquad (16)$$

Eq. (16) indicates that, interestingly, one may obtain the effective equations of motion, *for any guiding path*, from the simple knowledge of the defining equation for the path, $d\mathbf{q}/ds$. As is usual in analytical mechanics, one may derive a differential equation in terms of solely $s(t)$, from typical rearrangements of Eq. (16):

$$\left[\left(\frac{d\mathbf{q}}{ds}\right)^{T}\left(\frac{d\mathbf{q}}{ds}\right)\right]\left(\frac{d^2 s}{dt^2}\right)$$
$$+ \left[\left(\frac{d\mathbf{q}}{ds}\right)^{T}\left(\frac{d^2\mathbf{q}}{ds^2}\right)\right]\left[2\left(\frac{ds}{dt}\right)-\left(\frac{ds}{dt}\right)^2\right]$$
$$- \left(\frac{d\mathbf{q}}{ds}\right)^{T}\nabla_{\mathbf{q}}V[\mathbf{q}(s)] = 0 \qquad (17)$$

According to Eq. (17), the restricted motion of a molecular system through a curve depends on the tangent and the curvature of the path, as well as on the gradient vector at a point of this path. If the tangent vector is normalized, Eq. (17) is simplified to:

$$\frac{d^2 s}{dt^2} = \left(\frac{d\mathbf{q}}{ds}\right)^{T}\nabla_{\mathbf{q}}V[\mathbf{q}(s)] \qquad (18)$$

Application to the IRC, NP, and RGF paths

So far, the algebraic developments performed in this work have been completely general. However, the main conclusions, and actual advantages, arising from the present formulation, might only be assessed through specific applications. Here we shall explain first how the dynamic equations for the previously worked IRC and NP cases may be derived, showing that they come up with much less effort than from previous formulations. Afterwards, the methodology will be applied to a new example, the guiding path determined by the reduced gradient following (RGF) algorithm, for which the effective one-dimensional dynamic equations will be obtained for the first time.

The derivation of the IRC RPH goes as follows. One first considers that the potential is expanded until second order with respect to $\Delta\mathbf{q}_0$. Then Eq. (9) is taken and s and p_s are replaced by u and p_u. Finally, one simply substitutes in Eq. (3), yielding the defining equation for the IRC RPH (Eq. (17) in Ref. [10]).

Equivalently, one may obtain the NP RPH if one takes Eq. (6) and substitutes it in Eq. (9), always under the assumption of a quadratic expansion of the potential energy. Equation (24) of Ref. [11] is readily obtained.

The generality of the present derivation may be further illustrated with the derivation of the reduced gradient following RPH. This type of path was introduced by Quapp [19] and further analysed by Bofill et al. [20]. In this path, the gradient vector at each point of the path has a constant direction. Mathematically this path is formulated as an implicit function:

$$\mathbf{r} - \frac{\mathbf{g}[\mathbf{q}(\tau)]}{|\mathbf{g}[\mathbf{q}(\tau)]|} = \mathbf{0} \qquad (19)$$

where $\mathbf{r}$ is an arbitrary unit vector corresponding to a previously selected direction, whereas τ plays now the role of the curve parameter. The RGF is actually a rigorous formulation of the old "distinguished coordinate method", i.e. a mathematically grounded form of the usual procedure taken in most quantum chemistry reaction-co-ordinate calculations. The tangent vector for the RGF curve is:

$$\left(\mathbf{I} - \mathbf{r}\mathbf{r}^{T}\right)\mathbf{H}[\mathbf{q}(\tau)]\frac{d\mathbf{q}(\tau)}{d\tau} = \mathbf{P}_{\mathbf{r}}^{T}\mathbf{H}[\mathbf{q}(\tau)]\frac{d\mathbf{q}(\tau)}{d\tau} = \mathbf{0}_{M-1} \qquad (20)$$

where the $\mathbf{P}_{\mathbf{r}}$ matrix is a rectangular matrix such that the columns of it form an orthonormalized basis set, orthogonal to the $\mathbf{r}$ vector, $\mathbf{I}$ is the identity matrix and $\mathbf{0}_{M-1}$ is the zeroed vector with dimension $M-1$. Now it is assumed that any point on the path can be represented as a Taylor series in τ, truncated to first order:

$$\mathbf{q}(\tau) = \mathbf{q}(\tau_0) + (\mathbf{r}|\mathbf{P}_{\mathbf{r}})\mathbf{b}\Delta\tau_0 + O(\Delta\tau_0) \qquad (21)$$

where $(\mathbf{r}|\mathbf{P}_{\mathbf{r}})$ denotes the matrix formed by the $\mathbf{r}$ vector and the $\mathbf{P}_{\mathbf{r}}$ matrix, the $\mathbf{b}$ vector is defined as:

$$\mathbf{b}^{T} = \left(1, \left(-\mathbf{A}^{-1}\mathbf{f}\right)_1, \ldots, \left(-\mathbf{A}^{-1}\mathbf{f}\right)_{M-1}\right)b_1 \qquad (22)$$

with $\mathbf{A} = \mathbf{P}_{\mathbf{r}}^{T}\mathbf{H}\mathbf{P}_{\mathbf{r}}$, $\mathbf{f} = \mathbf{P}_{\mathbf{r}}^{T}\mathbf{H}\mathbf{r}$, whereas the b_1 constant is determined by normalization. At this point, the RGF RPH equations may then be readily obtained, just by using Eq. (15) and proceeding as in the previous IRC and NP cases:

$$H(\tau, p_\tau) = \frac{1}{2}p_\tau^2 + V_0 + \sqrt{\mathbf{g}_0^T\mathbf{g}_0}\,b_1\Delta\tau_0$$
$$+ \frac{1}{2}\Delta\tau_0^2 \mathbf{b}^{T}(\mathbf{r}|\mathbf{P}_{\mathbf{r}})^{T}\mathbf{H}(\mathbf{r}|\mathbf{P}_{\mathbf{r}})\mathbf{b} \qquad (23)$$

The Hamiltonian (Eq. 23) ends the formal section of the paper. Just note in passing that generating the RPH from the RGF following algorithm yields a nice connection with the reaction surface Hamiltonian (RSH) of Carrington and Miller [6]. To see this, one has to take two non-zero components of the **r** vector, since then one readily shows that the surface spanned by this two components is completely equivalent to the surface generated by the two large amplitude motions in the RSH treatment of Carrington and Miller.

Some numerical results

The reaction path approach has been tested to some extent in the past, both concerning "structural" descriptions of reactive processes (see, for example Ref. [21]) and the associated dynamics under several variants of the reaction-path Hamiltonian [22, 23, 24, 25, 26, 27]. Among the studies so far performed, outstanding numerical results were obtained by Yamashita and Miller in their test of the autocorrelation function approach for the rate constant, for the $3D$ H + H$_2$ system [28]. In particular, they obtained a correction factor for transition state theory in quite good agreement with exact close coupling calculations. Other notable numerical results were obtained by Billing in a series of papers [29, 30, 31, 32, 33], where an alternative formulation, based on the use of the second quantization approach for the perpendicular harmonic modes, was derived and tested. Furthermore, particularly convincing has been his recent reaction path rate constant calculation for the CH$_4$ + H reaction [34], for which a $12D$ exact quantum scattering calculation, augmented to $15D$ by means of the J-shifting approach [35] and further corrected by a more accurate evaluation of partition functions [36], served as an excellent benchmark. RP results lie very close to exact ones at low temperatures, the agreement being slightly worse (although always within an order of magnitude) at higher temperatures. A review on several aspects of the reaction path approach has recently been published by Kraka [1].

Most of the above numerical studies focus on two quite distinct aspects. On one hand, most mechanisms of chemical reactions are studied up to the reaction path topological features, plus the dependence on the reaction path of the frequencies associated with the perpendicular vibrational modes. On the other, as stated, several (but not too many) works focus on rate constant calculations. In other words, the available tests are based on either structural–like parameters or on rather averaged dynamic quantities. Given the nature of the present work, where general criteria for selecting specific reaction paths have been provided, it seems that more detailed tests, concerning the dynamics, should become available. In our opinion, an adequate test in this regard, i.e. on the accuracy of the reaction path approach, may be performed by testing how individual reaction path trajectories compare with those obtained from exact classical mechanics. This is, in principle, a rather stringent test, because the reaction path idea actually exploits the fact that trajectories should follow, *on average*, an imaginary path which is expected to be close to one of the specific choices for the reaction path [27]. Thus, individual collisions might clearly depart from exact solutions and this might not be an indicator of an important weakness of the method. But, in any case, it is clear from the outset that knowing the accuracy of the reaction path approach, from a comparison to exact dynamics, should enable more precise knowledge of the capabilities of the method.

Here we have used the well-known Müller-Brown $2D$ potential energy surface (PES) for such test. It is a PES that has been used throughout in many instances, being considered a rather good model potential for isomerization processes. Contour plots of this PES may be found elsewhere [11, 27]. Exact trajectories were integrated by a standard numerical integrator, whereas the RP trajectories were obtained by choosing the IRC path as the reaction path, so that the original (Cartesian) positions, as a function of time, were derived from Eq. (3), whereas the Cartesian momenta were obtained from the expression:

$$\mathbf{p}(u, p_u) = \frac{u^{\mathbf{H}_0 - \mathbf{1}}\mathbf{g}_0}{\mathbf{g}_0^T u^{2(\mathbf{H}_0 - \mathbf{1})}\mathbf{g}_0} p_u \qquad (24)$$

Figures 1 and 2 show the phase space parametric plots for the IRC–RPH and exact cases, for the (x, p_x) and (y, p_y) cases, respectively. Trajectories have been chosen to correspond to IRC–type initial conditions: motion with very low kinetic energy, with initial conditions given by the same initial point and momenta directions as those used in an IRC-following of the PES, i.e. the direction of the gradient vector corresponding to the imaginary frequency.

Figures 1 and 2 evidence, as expected, agreement between the IRC-RPH and the exact classical dynamics that, while being good on average, shows discrepancies in some portions (i.e. time intervals) of the trajectory. In particular, the (x, p_x) projection of the trajectory, Fig. 1, shows that, initially, the exact case runs with decreasing x value, but having essentially opposite momentum to the IRC–RPH case. It is then clear that, in this region of the PES, moving with a given velocity leads to a clear departure from the zero kinetic energy path. However, the averaged nature of the IRC translates into convergence in this trajectory for larger times. Well before the first vibrational period is finished (the vibrational half-periods may be identified from the local maxima and minima in the phase space plot), both the exact and IRC–RPH cases show good agreement, although it becomes slightly worse for the last stages of the trajectory shown in Fig. 1.

Figure 2 shows the (y, p_y) projection of the same trajectory as in Fig. 1. The overall agreement is qualitatively better than the (x, p_x) case, but it is
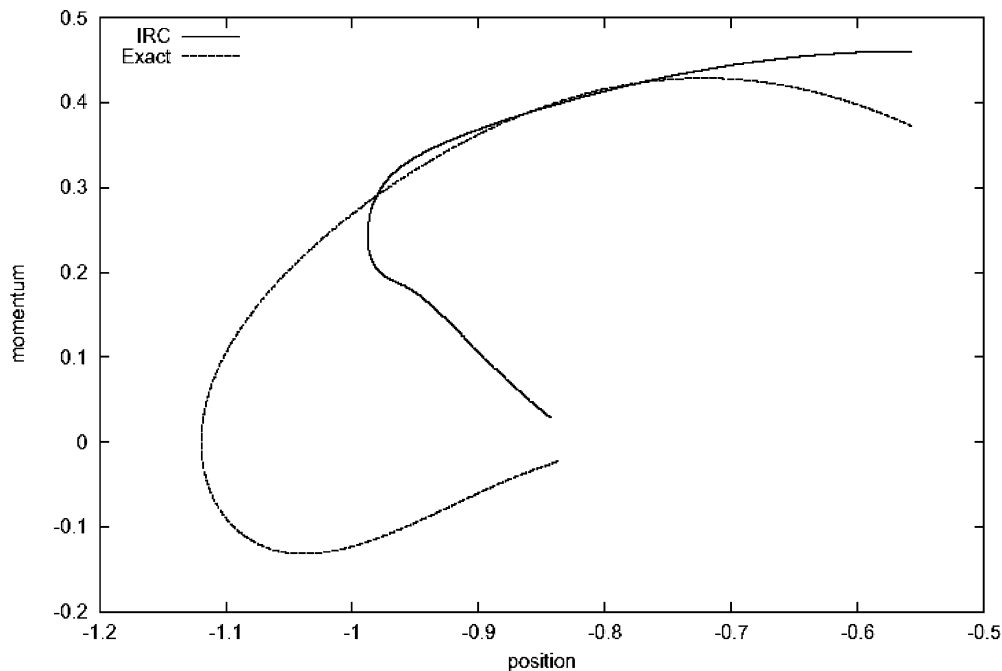
Fig. 1. A trajectory in the (x,p_x) phase space section computed using Müller–Brown 2D PES. This trajectory was started at the transition state, which is located at $x = -0.822$ Å, $y = 0.624$ Å, with a initial energy of 7 μhartree above the transition state energy (so it amounts to 1.75% of the barrier energy). The *solid line* corresponds to the trajectory obtained from the IRC–RPH, after using the transformation given in Eqs (3) and (24). The *dashed line* corresponds to the standard integration of the 2D, complete Hamilton equations of motion
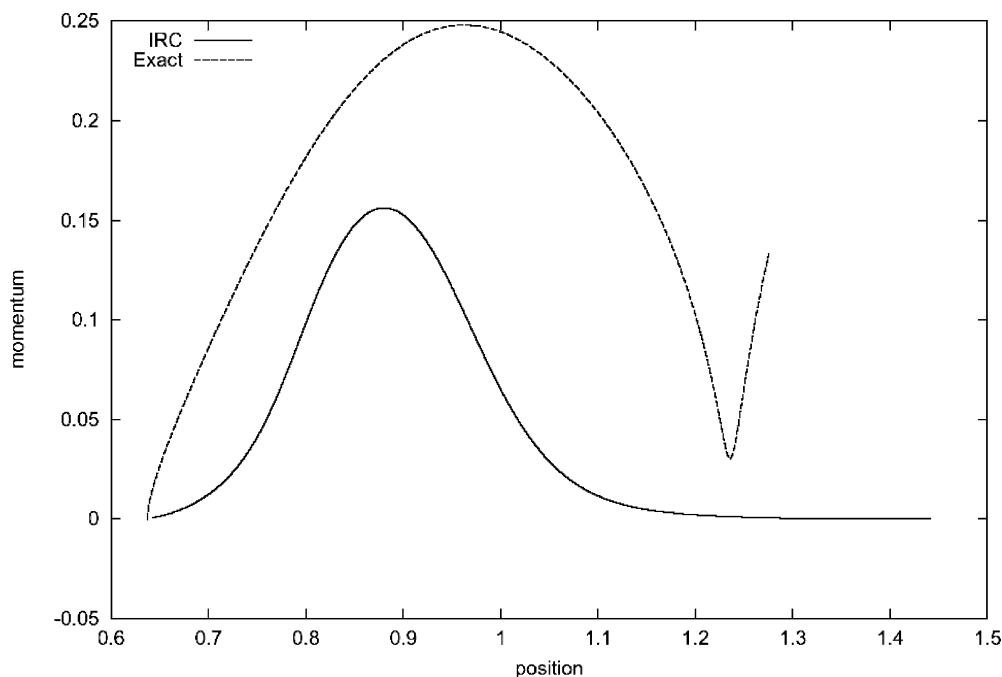

**Fig. 2.** The same as Fig. 1 for the (y,p_y) phase space section

quantitatively worse than that in Fig. 1. In addition, a turning point at long times is shown by the exact trajectory, which is not reproduced by the IRC–RPH case. This is the only qualitative feature, corresponding to exact trajectories, not reproduced by the RPH method, in the scanning of initial conditions performed for the present work.

Figures 1 and 2 correspond, actually, to very detailed analyses. Thus the emergence of discrepancies between the exact and the IRC–RPH time dependencies is not

surprising if one considers the respective levels of theory in which both formulations are based. Remarkably, however, things get more reasonable when one combines the x and y projections and plots the actual trajectory in configuration space. This is shown in Fig. 3. It is clearly evident that, in this case, the qualitative behaviour of both trajectories is essentially similar, i.e. both cases display a very similar vibration, encountering the first turning point at essentially the same times, in a given region of configuration space. The further progression in
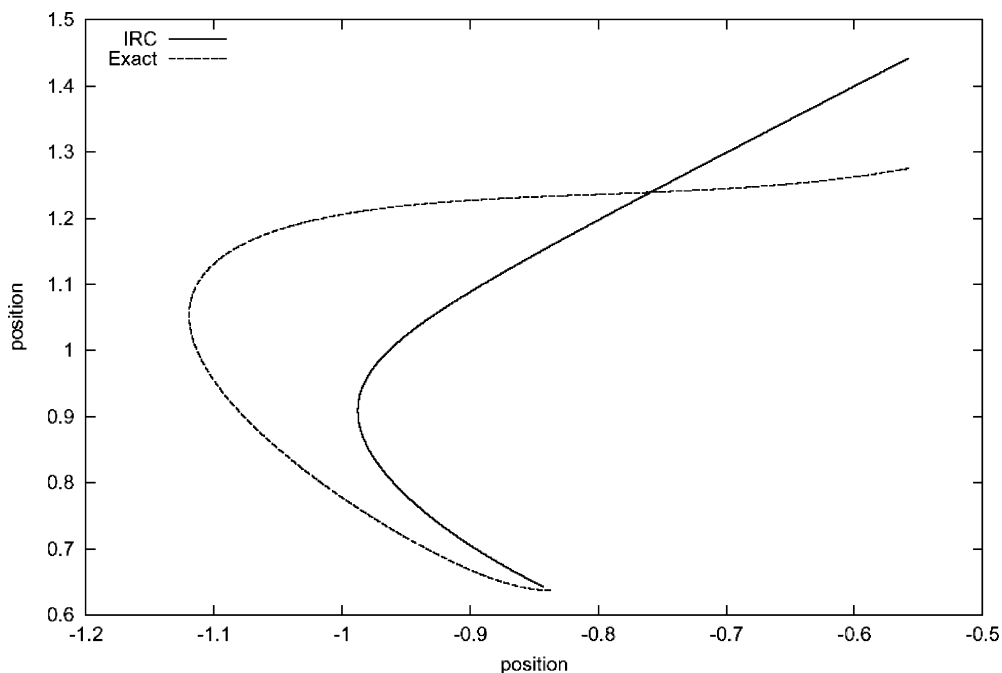
Fig. 3. The same trajectory as in Fig. 1 and 2, plotted in configuration space. The horizontal axis corresponds to the x coordinate, whereas the vertical axis corresponds to the y coordinate
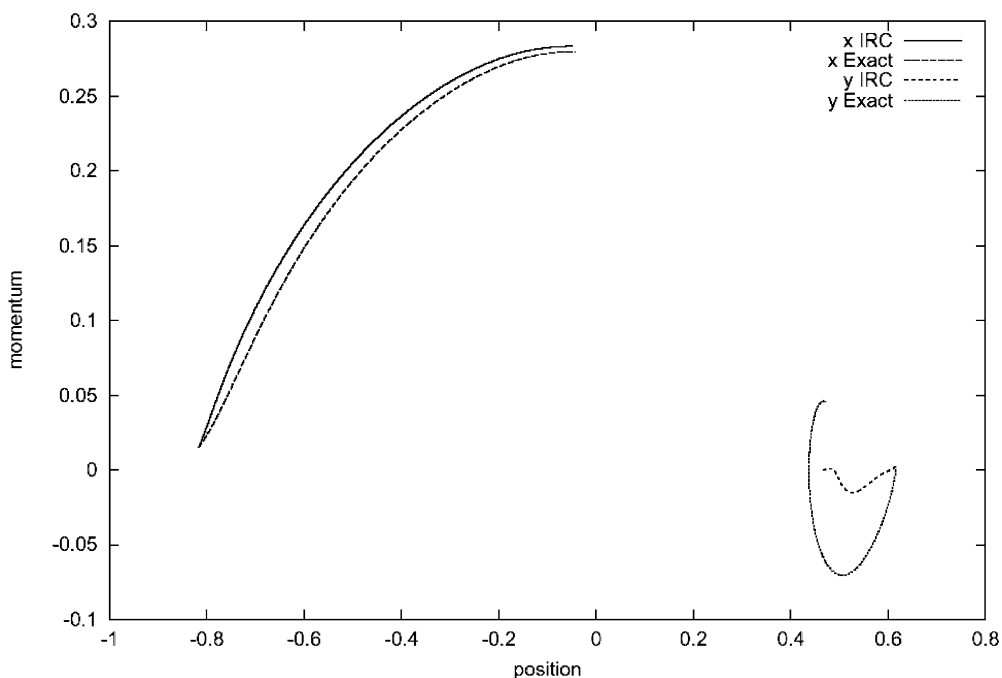
Fig. 4. Composition of the phase space (x,p_x) and (y,p_y) projections of a trajectory started at the same PES location as that shown in Fig. 1, 2, and 3 (i.e. the transition state in the Müller–Brown 2D potential) but having the opposite momentum

time is also quite similar, ending at locations which appear quite close on the PES.

Actually, all cases so far studied (a larger group of trajectories having small initial momenta, not shown here) give rise to a semi-quantitative match between the IRC-RPH and the exact dynamics. This feature may be assessed from inspection of Fig. 4, where the phase space plots for both the (x,p_x) and (y,p_y) projections, for a trajectory having opposite momentum to that shown in Figs. 1 and 2, are shown in the same panel. Good

agreement is obtained between the exact and RPH cases, for the x projection, although they are much worse for the y case. Nevertheless, the qualitative features of the exact trajectories are essentially reproduced in Fig. 4.

Overall, results appear quite interesting, putting an additional amount of confidence, besides previous work on rate constant calculations, on the possibility of using the RPH for rather accurate, physically meaningful descriptions of complex chemical processes. It has the enormous advantage of avoiding the knowledge of large

portions of the PES and, most notably, of avoiding the terribly tedious stage of fitting the available information on the PES to a suitably behaved interpolating analytical function.

Summary and conclusions

A rigorous mathematical criterion for deriving the reaction-path Hamiltonian from a general reference path has been provided in the present work. Resting on Noether's theorem on the integrability of the Lagrange equations over differentiable varieties, it is shown that the only criterion is that the reference path, defined in terms of its dependence on a freely chosen parameter, must not explicitly depend on this parameter.

The above result opens the possibility of deriving, in a straightforward manner, dynamic equations related to the reaction-path parameter and its conjugated linear momentum, knowing by construction that the Bernouilli–type differential equation is readily transformable to the corresponding dynamic equations in Hamiltonian form. One thus ensures conservation of total energy, irrespective of the kind of dimensionality reduction being performed, as one passes from the full $3N$–dimensional description to the $1D$ reaction path problem. Interestingly, as has been stated elsewhere [10], this $1D$ path leads to equivalence with the brachistochrone problem, thus yielding the Bernouilli-type differential equation.

The feasibility in obtaining the dynamic equations, from any suitable starting path, is shown by explicitly discussing how the IRC and the NP RPH are derived under the new theoretical framework, these two cases having been studied in previous work by the authors. This framework has been further tested in the straightforward derivation of the dynamic equations associated with an RGF path, for the first time. It is hoped that this flexibility will find instrumental use in the study of the reaction dynamics of very complex systems, for which involved reaction paths are expected to appear in their accurate description.

Finally, a numerical, stringent test of the RPH methodology has been performed, by comparing individual trajectories obtained from the RPH dynamic equations and those from exact classical mechanics. Interestingly, rather good overall qualitative agreement has been obtained between the RP and exact phase space trajectory plots, for all initial conditions explored by the authors. This result provides additional experience on the capabilities of the RP idea, accumulating more confidence on the possibility of performing accurate dynamics studies of complex molecular systems.

References

1. Kraka E (1998) In: Schleyer PvR (ed) Encyclopedia of computational chemistry. Wiley, New York, p 2437
2. Billing GD, Mikkelsen KV (1997) Advanced molecular dynamics and chemical kinetics. Wiley, New York
3. Schatz GC, Ratner MA (1993) Quantum mechanics in chemistry. Prentice Hall, New York
4. Miller WH, Handy NC, Adams JE (1980) J Chem Phys 72:99
5. Miller WH (1983) J Phys Chem 87:3811
6. Carrington T Jr, Miller WH (1984) J Chem Phys 81:3942
7. Billing GD (1996) Mol Phys 89:355
8. Koch A, Billing GD (1997) J Chem Phys 107:7242
9. Colletti C, Billing GD (1999) Phys Chem Chem Phys 1:4141
10. González J, Giménez X, Bofill JM (2001) J Phys Chem A 105:5022
11. González J, Giménez X, Bofill JM (2002) J Chem Phys 116:8713
12. (a) Hofacker GL (1963) Z Naturforsch 18a: 607; (b) Marcus RA (1966) J Chem Phys 45:4493; (c) Marcus RA (1968) J Chem Phys 49:2610; (d) Marcus RA (1968) J Chem Phys 49:2617; (e) Hofacker GL, Levine RD (1975) Chem Phys Lett 33:2769
13. Fukui K (1981) Acc Chem Res 14:363
14. González C, Schlegel HB (1990) J Phys Chem 94:5523
15. Quapp W, Heidrich D (1984) Theor Chim Acta 66:245
16. Quapp W, Hirsch M, Heidrich D (1998) Theor Chim Acta 100:285
17. Courant R, Hilbert D (1950) Methods in mathematical physics. Wiley, New York
18. Arnold VI (1997) Métodos matemáticos de la mecánica clásica. Mir, Moscow (Spanish translation of the 1984 Russian edition)
19. Quapp W, Hirsch M, Imig O, Heidrich D (1998) J Comput Chem 19:4087
20. Crehuet R, Bofill JM, Anglada JM (2002) Theor Chim Acta 107:130
21. Cui Q, Karplus M (2002) J Phys Chem B 106:1768
22. (a) Fang JY, Hammes–Schiffer S (1998) J Chem Phys 108:7085; (b) Fang JY, Hammes–Schiffer S (1998) J Chem Phys 109:7051
23. Nguyen KA, Jackels CF, Truhlar DG (1996) J Chem Phys 104:6491
24. Song K, Peslherbe GA, Hase WL, Dobbyn AJ, Stumpf M, Schinke R (1995) J Chem Phys 103:8891
25. Taketsugu T, Gordon MS (1996) J Chem Phys 104:2834
26. Okuno Y (2000) J Chem Phys 113:3130
27. González J, Giménez X, Bofill JM (2002) Phys Chem Chem Phys 4:2921
28. Yamashita K, Miller WH (1985) J Chem Phys 82:5475
29. Billing GD (1984) Chem Phys 89:199
30. Billing GD (1989) Chem Phys 135:423
31. Billing GD (1990) Chem Phys 146:63
32. Billing GD (1992) Chem Phys 159:109
33. Billing GD (1992) Chem Phys 161:245
34. Billing GD (2002) Chem Phys 277:325
35. (a) Huarte-Larrañaga F, Manthe U (2000) J Chem Phys 113:5115 (2000); (b) Huarte-Larrañaga F, Manthe U (2001) J Phys Chem A 105: 2522; (c) Huarte-Larrañaga F, Manthe U (2002) J Chem Phys 116:2863
36. Bowman JM, Wang D, Huang X, Huarte-Larrañaga F, Manthe U (2001) J Chem Phys 114:9683